

# Compressed FEC Codes With Spatial-Coupling

Chulong Liang, Junjie Ma, and Li Ping, *Fellow, IEEE*

**Abstract**—An error floor problem is observed for a spatially coupled sparse-regression (SCSR) code with limited sparsity in low-to-medium rates. This letter presents a scheme that also involves spatial-coupling and compressed-sensing (SCCS) similar to SCSR. We replace position modulation in SCSR by a general concatenated forward error control code. We introduce a chaining principle that improves the error floor behavior of the underlying code. We show that SCCS based on chained Hadamard codes can offer significantly improved performance.

**Index Terms**—Approximate message passing (AMP), compressed sensing, concatenated codes, Hadamard codes, message passing decoding, sparse-regression (SR) codes, spatial coupling (SC), turbo codes.

## I. INTRODUCTION

IN A compressed-sensing system, the sparsity of the transmitted signal can be exploited to carry information using position modulation. This is the principle of the recently proposed sparse-regression (SR) codes [1]–[10]. It is shown that a spatially-coupled SR (SCSR) code can potentially achieve the channel capacity [11], [12]. However, asymptotically high sparsity is required for capacity achieving performance with SCSR. In practice, sparsity has to be limited since decoding complexity for position modulation increases with sparsity. We observed that the performance of an SCSR code is not satisfactory for modest sparsity in low-to-medium rate regions.

In this letter, we present a scheme that also involves spatial-coupling and compressed-sensing (SCCS). We show the equivalence between SCSR based on position modulation and SCSR based on standard binary Hadamard codes. We replace position modulation using a concatenated code. We then introduce a chaining principle that improves the error floor behavior of the underlying code.

The results presented in this letter provide useful insights into the SCSR and the related schemes [13].

- Compression can be applied to an FEC code, which provides flexibility in continuous rate adjustment. This scheme is robust under random puncturing, since the latter is a natural consequence of random compression. It also results in Gaussian-like signaling, which is optimal for channels corrupted by additive Gaussian noise.
- Spatial-coupling is important to maintain good decoding performance. This follows the analysis in [14]–[17] for

Manuscript received November 7, 2016; revised December 23, 2016; accepted January 14, 2017. Date of publication January 16, 2017; date of current version May 6, 2017. The work described in this paper was jointly supported by grants from University Grants Committee of the Hong Kong SAR, China (Project No. AoE/E-02/08, CityU 11217515 and CityU 11280216). The associate editor coordinating the review of this letter and approving it for publication was C. Feng.

C. Liang and L. Ping are with the Department of Electronic Engineering, City University of Hong Kong, Hong Kong (e-mail: chuliang@cityu.edu.hk; eliping@cityu.edu.hk).

J. Ma was with the Department of Electronic Engineering, City University of Hong Kong, Hong Kong. He is now with the Department of Statistics, Columbia University, New York, NY 10027-6902 USA (e-mail: junjiema2-c@my.cityu.edu.hk).

Digital Object Identifier 10.1109/LCOMM.2017.2655055

coupling over the binary field and in [13], [18], [19] over the real field.

- The position modulation in SCSR can be replaced by a general FEC code. The performance of the underlying code (before compression) is crucial for the overall performance.

We will show that SCCS based on chained Hadamard codes and turbo codes can offer significantly performance enhancement over SCSR. The resultant codes are universally good over a certain range of random puncturing. This is verified by both evolution and simulation methods.

## II. SCSR CODES

In this section, we briefly outline the structure of SCSR codes. We will verify the equivalence between position modulation and binary modulation. This provides a useful basis for the discussion in the next section.

### A. Hadamard Code and Position Modulation

Denote by  $\mathbf{H}$  a size  $N \times N$  Hadamard matrix in the binary phase shift keying (BPSK) format [20] with normalized column weights. The  $N$  columns  $\{\mathbf{h}_i\}$  of  $\mathbf{H}$  form an Hadamard code. The related encoding is specified by a one-to-one mapping  $\mathbf{d} \leftrightarrow \mathbf{h}_i$ , where  $\mathbf{d}$  is a set of  $n$  binary bits and  $N = 2^n$ .

Denote by  $\mathbf{e}_i$  a length- $N$  unity vector with a non-zero entry at position  $i$ :  $\mathbf{e}_i = [0, \dots, 0, 1, 0, \dots, 0]^T$ . We call the collection of  $N$  unity vectors  $\{\mathbf{e}_i\}$ ,  $i = 1, 2, \dots, N$ , a position modulation (PM) code. The encoding process is specified by a one-to-one mapping  $\mathbf{d} \leftrightarrow \mathbf{e}_i$ . It can be shown that  $\mathbf{h}_i$  and  $\mathbf{e}_i$  form an Hadamard transform pair:

$$\mathbf{H}\mathbf{h}_i = \mathbf{e}_i \text{ and } \mathbf{H}\mathbf{e}_i = \mathbf{h}_i. \quad (1)$$

Due to the orthogonality of  $\mathbf{H}$ , for any  $(i, j)$  pair,

$$\|\mathbf{e}_i - \mathbf{e}_j\|^2 = \|\mathbf{h}_i - \mathbf{h}_j\|^2. \quad (2)$$

Eqn. (2) indicates that a PM code has the same distribution of Euclidean distances as a corresponding Hadamard code. Thus they have the same code structure in two different formats.

### B. Parallel Hadamard Codes and Parallel PM Codes

Let  $\mathbf{d}$  be a binary information sequence of length  $J \times n$ . We segment  $\mathbf{d}$  into  $J$  sections with equal length of  $n$  and apply Hadamard encoding to each section. The collection of  $J$  Hadamard codewords form a parallel Hadamard (PH) code. Similarly, we define a parallel PM (PPM) code as the section-wise Hadamard transform of a PH code.

### C. SCSR Codes

An SCSR code is defined as follows [11]. Let  $\mathbf{d} = \{\mathbf{d}^{(k)}\}$ ,  $k = 1, 2, \dots, K$ , be  $K$  binary information sequences, each of length  $J \times n$ . We encode each  $\mathbf{d}^{(k)}$  to  $\mathbf{c}^{(k)}$  using a PPM

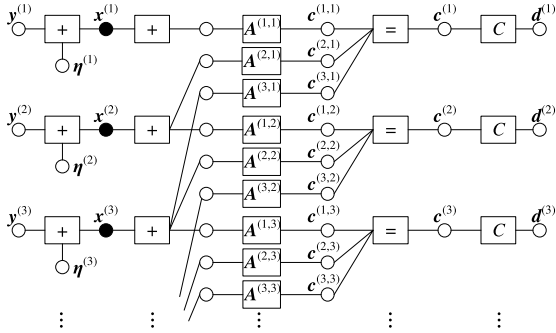


Fig. 1. The structure of an SCSR code with  $W = 3$ . The addition is performed in the real domain.

code  $C$ . We arrange  $\{\mathbf{c}^{(k)}\}$  as a column vector  $\mathbf{c}$  and apply a sensing matrix  $A$  to  $\mathbf{c}$ , results in an SCSR codeword

$$\mathbf{x} = \mathbf{Ac}. \quad (3)$$

In particular, (4) shows a block bandlimited structure of  $A$  with block bandwidth  $W$ , where each non-zero sub-block is denoted by  $A^{(w,k)}$ . It is shown in [11] and [15] that such a bandlimited structure results in the spatial-coupling effect.

$$\begin{bmatrix} \mathbf{x}^{(1)} \\ \vdots \\ \mathbf{x}^{(K-1)} \\ \mathbf{x}^{(K)} \\ \vdots \\ \mathbf{x}^{(K+W-1)} \end{bmatrix} = \begin{bmatrix} A^{(1,1)} & & & & \mathbf{0} \\ \vdots & \ddots & & & \\ A^{(W,1)} & \ddots & A^{(1,K)} & & \\ & \ddots & \vdots & \ddots & \\ & & A^{(W,K)} & \ddots & A^{(1,K)} \\ & & & \ddots & \vdots \\ \mathbf{0} & & & & A^{(W,K)} \end{bmatrix} \begin{bmatrix} \mathbf{c}^{(1)} \\ \vdots \\ \mathbf{c}^{(K)} \\ \vdots \\ \mathbf{c}^{(K)} \end{bmatrix} \quad (4)$$

Fig. 1 is an illustration for (4) with  $W = 3$ . Each  $\mathbf{d}^{(k)}$  is encoded using  $C$  into  $\mathbf{c}^{(k)}$ . Each  $\mathbf{c}^{(k)}$  is repeated into  $W$  replicas  $\{\mathbf{c}^{(w,k)}\}$  in the block labeled by “=”. Each section  $\mathbf{x}^{(k)}$  of  $\mathbf{x}$  is the linear combination of  $A^{(w,k)} \mathbf{c}^{(w,k)}$  in the neighboring  $W$  copies. Here a copy loosely refers to the collection of  $\mathbf{d}^{(k)}, \{\mathbf{c}^{(w,k)}\}$  and  $\mathbf{x}^{(k)}$ . Let

$$\mathbf{y}^{(k)} = \mathbf{x}^{(k)} + \boldsymbol{\eta}^{(k)}, \quad (5)$$

where  $\mathbf{y}^{(k)}$  is a noisy observation of  $\mathbf{x}^{(k)}$  and  $\boldsymbol{\eta}^{(k)}$  contains independent identically distributed (IID) Gaussian variables.

Let the size of each  $A^{(w,k)}$  be  $(\alpha JN) \times (JN)$ , where  $0 \leq \alpha \leq 1$  is the compression ratio. We will assume that the same compression ratio is applied to all sub-blocks  $\{A^{(w,k)}\}$ .

#### D. Equivalence Between PH and PPM Formats

We adopt the decoding method in [11] based on approximate message passing (AMP) [21]. It involves the iteration of a linear estimator and a non-linear estimator. The coding constraint is ignored in the former and is handled in a section-by-section way in the latter. Here a section is defined in Section II-B as a PM code for a standard SCSR code [11].

Now consider replacing each section of a PM code by a corresponding Hadamard code. From state evolution (SE) analysis [11], the performance of AMP based detection algorithm remains unchanged if

- the sensing matrix remains unchanged and
- the mean square error (MSE) of the section-by-section non-linear estimator remains unchanged.

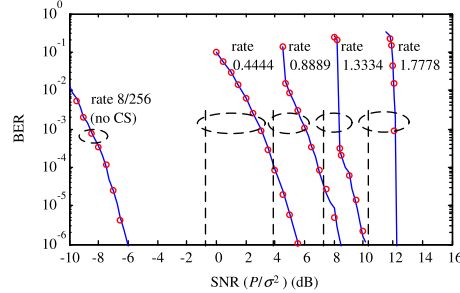


Fig. 2. Performance of SCSR codes. Vertical dashed lines are for Gaussian capacities, solid lines for PPM format and circle for PH format.

Recall from (2) that PH and PPM have exactly the same distance distribution. Therefore their performance, in terms of either bit-error rate (BER) or MSE is the same under optimal decoding (which is the case for each section). Based on this fact, it can be shown that using a PH code or a corresponding PPM code for  $C$  results in exactly the same performance. This will be verified by the example below.

#### E. Simulated Performance

Fig. 2 shows the simulated performance of SCSR codes in both PH and PPM formats with the following parameters:  $N = 256$ ,  $J = 2048$ ,  $W = 3$  and  $K = 16$ . In this letter, the signal-to-noise ratio (SNR) is defined as in [11]. Each  $A^{(w,k)}$  is generated using randomly selected rows from an  $N_H \times N_H$  Hadamard matrix. In the limiting case of infinite  $J$  and  $N$ ,  $A^{(w,k)}$  and  $A^{(w',k')}$  are uncorrelated for different  $w$ ,  $w'$ ,  $k$ , and  $k'$ . For finite  $J$  and  $N$ , however, this is not guaranteed. To reduce correlation, random row and column interleaving are applied to each  $A^{(w,k)}$ . Following [11], AMP can be used for decompressor. We also find that orthogonal AMP (OAMP) [22] can be more robust in some situations. Slight modified OAMP is used for the spatially-coupled scheme similar to that in [23]. Fast Hadamard transform (FHT) is used in OAMP with complexity  $\log_2(N_H)$  per bit. Iteration proceeds until convergence. To reduce cost, each copy of length  $= J \times N = 524288$  is partitioned into 8 segments with length 65536 each. Each segment is individually compressed. This is based on our experimental observation that performance stabilizes for  $N_H > 65536$ . From Fig. 2, we can see that SCSR codes have the same performance in two formats as expected.

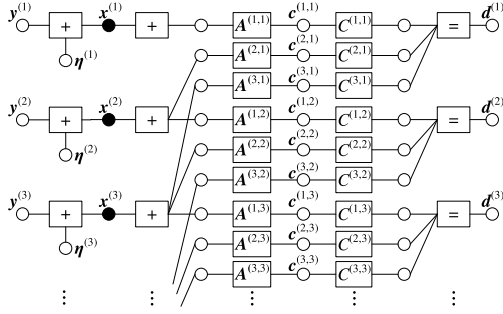
The performance in Fig. 2 is good at high rates. However, an error floor problem appears for rates below 1.5. The problem is related to the poor coding gain of the underlying length-256 Hadamard code. We will introduce a solution to the problem in the next section.

### III. SCCS CODES

#### A. Spatially-Coupled Compressed-Sensing Scheme

Consider the spatially-coupled compressed-sensing (SCCS) coding scheme in Fig. 3. The notations in Fig. 3 are the same as those in Fig. 1 except the following differences.

- In SCSR, each  $\mathbf{d}^{(k)}$  is encoded only once. The resultant  $\mathbf{c}^{(k)}$  is repeated for  $W$  times.
- In SCCS, each  $\mathbf{d}^{(k)}$  is repeated  $W$  times. Each replica is independently interleaved and then encoded. This results in a turbo coding effect [24].

Fig. 3. The structure of the SCCS coding scheme with  $W = 3$ .

Similar to (4), we can represent Fig. 3 in the matrix form as

$$\begin{bmatrix} \mathbf{x}^{(1)} \\ \mathbf{x}^{(2)} \\ \mathbf{x}^{(3)} \\ \vdots \end{bmatrix} = \begin{bmatrix} \mathbf{A}^{(1,1)} & \mathbf{0} & \mathbf{0} & \mathbf{A}^{(1,2)} & \mathbf{0} & \mathbf{0} & \cdots \\ \mathbf{0} & \mathbf{A}^{(2,1)} & \mathbf{0} & \mathbf{A}^{(2,2)} & \mathbf{0} & \mathbf{0} & \cdots \\ \mathbf{0} & \mathbf{0} & \mathbf{A}^{(3,1)} & \mathbf{0} & \mathbf{A}^{(3,2)} & \mathbf{0} & \cdots \\ \mathbf{0} & \mathbf{0} & \mathbf{0} & \mathbf{A}^{(3,2)} & \mathbf{0} & \mathbf{0} & \cdots \\ \vdots & \vdots & \vdots & \vdots & \vdots & \vdots & \ddots \end{bmatrix} \begin{bmatrix} \mathbf{c}^{(1,1)} \\ \mathbf{c}^{(2,1)} \\ \mathbf{c}^{(3,1)} \\ \mathbf{c}^{(1,2)} \\ \mathbf{c}^{(2,2)} \\ \mathbf{c}^{(3,2)} \\ \vdots \end{bmatrix} \quad (6)$$

#### B. Chained Hadamard and Chained PM Codes

To further enhance performance, we adopt a chaining principle for each  $C^{(w,k)}$  as follows.

For simplicity, let  $K = 1$  and so  $\mathbf{d} = \mathbf{d}^{(k)}$ . We segment  $\mathbf{d}$  into  $J$  sections denoted as  $\{\mathbf{d}_j\}$ . Each section  $\mathbf{d}_j$  consists of  $n$  bits  $\mathbf{d}_j = \{d_{j,n'}\}$ , based on which we define a state variable  $s_j$  as

$$s_j = \sum_{j'=1}^j p_{j'} = s_{j-1} + p_j \quad (7)$$

with  $s_0 = 0$ , where  $p_j = \sum_{n'=1}^n d_{j,n'}$ . A chained Hadamard (CH) code has  $J$  sections  $\{\mathbf{c}_j\}$ . Assume that the  $j$ th data section  $\mathbf{d}_j \leftrightarrow \mathbf{h}_i$  under the mapping for the Hadamard code. Then the  $j$ th coded section,

$$\mathbf{c}_j = \begin{cases} \mathbf{h}_i, & \text{if } s_{j-1} = 0, \\ -\mathbf{h}_i, & \text{if } s_{j-1} = 1. \end{cases} \quad (8)$$

Similarly, a chained PM (CPM) code is defined by replacing  $\mathbf{h}_i$  with  $\mathbf{e}_i = \mathbf{H}\mathbf{h}_i$  in (8).

A chained code (with CH or CPM) can be seen as obtained by chaining the sections of a corresponding parallel code using the state variables  $\{s_j\}$ . The above chaining principle can be applied to each copy when  $K > 1$ .

The above encoding method is equivalent to the zigzag Hadamard code introduced in [20] in the non-systematic form. Chaining and concatenation can significantly reduce the occurrence probability of codewords with small weights. The related advantages can be analyzed using the distance spectrum as discussed in [20].

#### C. Iterative Detection and Evolution Analysis

Fig. 4 illustrates the principle of message passing decoding for an SCCS code. For simplicity, only the part corresponding to  $C^{(w,k)}$  is shown. The messages in Fig. 4 are defined as follows. A rightward message  $(\bar{\mathbf{c}}^{(w,k)}, \bar{\mathbf{v}}^{(w,k)})$  is the mean

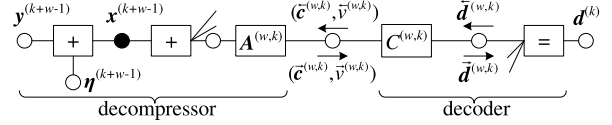
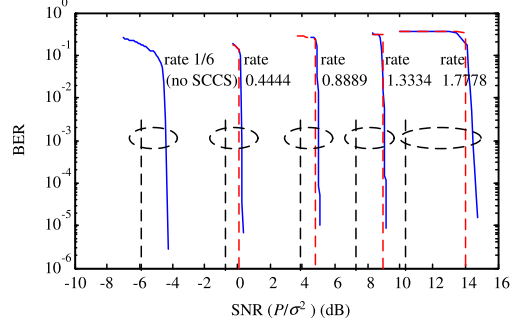
Fig. 4. Illustration of message passing corresponding to  $C^{(w,k)}$  of an SCCS code.

Fig. 5. Performance of SCCS codes based on CH coding. Vertical dashed lines are for Gaussian capacities, solid lines for simulation and dashed lines for state evolution.

and variance pair for  $\mathbf{c}^{(w,k)}$  computed at decompressor based on AMP (or OAMP). The detailed computation rules can be found in [9], [11], [12], [21]–[23]. A corresponding leftward message  $(\bar{\mathbf{c}}^{(w,k)}, \bar{\mathbf{v}}^{(w,k)})$  is the mean and variance pairs of  $\mathbf{c}^{(w,k)}$  computed from the log-likelihood ratios (LLRs) at the decoder for  $C^{(w,k)}$ . The messages  $\bar{\mathbf{d}}^{(w,k)}$  and  $\bar{\mathbf{d}}^{(w,k)}$  are, respectively, the extrinsic LLRs for  $\mathbf{d}^{(k)}$  generated by the decoder for  $C^{(w,k)}$  and the repetition constraint (a block labeled by “=”). The related operations are similar to those for turbo [24] and LDPC codes [14]–[17].

Denote by  $I(\bar{\mathbf{d}}^{(w,k)})$  the mutual information between  $\bar{\mathbf{d}}^{(w,k)}$  and  $\mathbf{d}^{(k)}$ . Similarly, we define  $I(\bar{\mathbf{d}}^{(w,k)})$ . We can define the transfer functions between messages for this purpose. For the decompressor, the transfer function between  $\bar{\mathbf{v}}^{(w,k)}$  and  $\bar{\mathbf{v}}^{(w,k)}$  is the same as that used in [11] (for AMP) or [23] (for OAMP) for the SCSR code. The transfer function between  $I(\bar{\mathbf{d}}^{(w,k)})$  and  $I(\bar{\mathbf{d}}^{(w,k)})$  is given by the  $J$ -function in [14]–[17], [25] for repetition codes. Finally, for  $C^{(w,k)}$ , we can generate a two-dimensional function using simulation, with inputs  $(\bar{\mathbf{v}}^{(w,k)}, I(\bar{\mathbf{d}}^{(w,k)}))$  and outputs  $(\bar{\mathbf{v}}^{(w,k)}, I(\bar{\mathbf{d}}^{(w,k)}))$ .

With these transfer functions, we can evaluate the performance of the above decoding process by tracking  $\bar{\mathbf{v}}^{(w,k)}, \bar{\mathbf{v}}^{(w,k)}, I(\bar{\mathbf{d}}^{(w,k)})$  and  $I(\bar{\mathbf{d}}^{(w,k)})$ . The process is in spirit similar to the extrinsic information transfer (EXIT) chart analysis [25]. It has been used in [14]–[17] for analyzing spatially coupled codes.

#### D. Numerical Results

Fig. 5 shows both simulated (solid lines) and state evolution (dashed lines) results for an SCCS code based on the following parameters: CH coding with  $n = 2, J = 8192, W = 3$  and  $K = 16$ . Each  $\mathbf{A}^{(w,k)}$  is generated using randomly selected rows from an Hadamard matrix of size  $N_H = 32768$ .

From Figs. 2 and 5, SCCS outperforms SCSR significantly at rates 0.4444 to 1.3334 in real channels (corresponding to 0.8888 to 2.6668 in complex channels), which covers

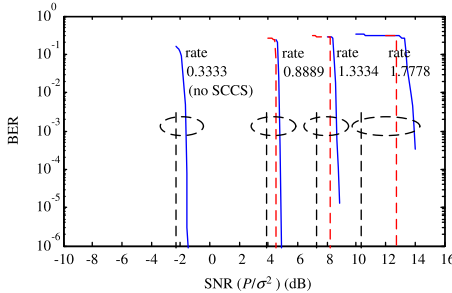


Fig. 6. Performance of SCCS codes based on turbo coding. Vertical dashed lines are for Gaussian capacities, solid lines for simulation and dashed lines for state evolution.

the typical rate range of common wireless communications. The advantage of SCCS attributes to the recursive nature of the chained encoders with random interleaving at their input. This produces interleaving gain as analyzed in [26]. SCCS remains good after a certain range of random puncturing, which demonstrates its good universality. However, SCCS has poor performance at high rates, about 2 dB degradation for the waterfall region. We are still investigating this issue. The state evolution matches reasonably well with simulation in the low BER region, except at rate = 1.7778 where the convergence of the SCCS decoder is poor. In addition, compared with SCSR in Fig. 2 with a PPM of size  $N = 256$ , SCCS in Fig. 5 has a much lower complexity ( $N = 2^n = 4$ ).

#### E. Other Underlying FEC Codes

The local codes  $\{C^{(w,k)}\}$  can be generated by other options. An example is shown in Fig. 6 based on the rate-1/3 (13, 15)8 turbo code [24]. This code can be separated into three parts: a systematic sequence  $\mathbf{d}$  and two parity-check sequences  $\mathbf{c}_1$  and  $\mathbf{c}_2$ . We set  $W = 3$ . Then  $C^{(w,k)}$  generates  $\mathbf{d}$  for  $w = 1$ ,  $\mathbf{c}_1$  and  $\mathbf{c}_2$  respectively for  $w = 2$  and 3. The first encoder is actually a trivial one that generates the systematic part of a turbo code. The other parameters are:  $K = 16$ , 16381 information bits per copy (with 3 more termination bits), each  $A^{(w,k)}$  generated using randomly selected rows from an Hadamard matrix of size  $N_H = 16384$ . We can see that this SCCS scheme based on a turbo code performs excellently in the low-to-medium rate region. However, its performance also deteriorates at high rate.

## IV. CONCLUSIONS

We presented an SCCS scheme based on compressed FEC codes, which provides flexible rate adjustment and Gaussian like signaling. SCCS can be seen as a modified SCSR scheme, with position modulation replaced by a general FEC code. We showed that concatenation and chaining techniques can be used to improve error floor performance in SCCS. We further show that SCCS based on a standard turbo code also offers impressive performance.

## REFERENCES

- [1] A. R. Barron and A. Joseph, "Toward fast reliable communication at rates near capacity with Gaussian noise," in *Proc. IEEE Int. Symp. Inf. Theory*, Austin, TX, USA, Jun. 2010, pp. 315–319.
- [2] I. Kontoyiannis, K. R. Rad, and S. Gitzenis, "Sparse superposition codes for Gaussian vector quantization," in *Proc. IEEE Inf. Theory Workshop*, Cairo, Egypt, Jan. 2010, p. 1.
- [3] E. Price, "Rateless codes approaching capacity of the Gaussian channel," [Online]. Available: <http://web.mit.edu/ecprice/Public/gaussian-channel.pdf>
- [4] A. R. Barron and S. Cho, "High-rate sparse superposition codes with iteratively optimal estimates," in *Proc. IEEE Int. Symp. Inf. Theory*, Cambridge, MA, USA, Jul. 2012, pp. 2696–2700.
- [5] M. Peleg and S. Shamai (Shitz), "On sparse sensing of coded signals at Sub-Landau sampling rates," in *Proc. IEEE 27th Conv. Elect. Electron. Eng. Israel (IEEJI)*, Nov. 2012, pp. 1–5.
- [6] E. G. W. Peters, "Sparse regression codes for networked control systems," M.S. thesis, Aalborg Univ., Aalborg, Denmark, Jun. 2013.
- [7] Y. Takeishi, M. Kawakita, and J. Takeuchi, "Least squares superposition codes with Bernoulli dictionary are still reliable at rates up to capacity," *IEEE Trans. Inf. Theory*, vol. 60, no. 5, pp. 2737–2750, May 2014.
- [8] R. Venkataraman, T. Sarkar, and S. Tatikonda, "Lossy compression via sparse linear regression: Computationally efficient encoding and decoding," *IEEE Trans. Inf. Theory*, vol. 60, no. 6, pp. 3265–3278, Jun. 2014.
- [9] C. Rush, A. Greig, and R. Venkataraman, "Capacity-achieving sparse regression codes via approximate message passing decoding," in *Proc. IEEE Int. Symp. Inf. Theory*, Hong Kong, Jun. 2015, pp. 2016–2020.
- [10] C. Condo and W. J. Gross, "Sparse superposition codes: A practical approach," in *Proc. IEEE Workshop Signal Process. Syst.*, Hangzhou, China, Oct. 2015, pp. 1–6.
- [11] J. Barbier, C. Schülke, and F. Krzakala, "Approximate message-passing with spatially coupled structured operators, with applications to compressed sensing and sparse superposition codes," *J. Statist. Mech. Theory Experim.*, vol. 2015, no. 5, p. P05013, May 2015.
- [12] J. Barbier, M. Dia, and N. Macris, "Proof of threshold saturation for spatially coupled sparse superposition codes," in *Proc. IEEE Int. Symp. Inf. Theory*, Barcelona, Spain, Jul. 2016, pp. 1173–1177.
- [13] C. Liang, J. Ma, and L. Ping, "Towards Gaussian capacity, Universality and short block length," in *Proc. 9th Int. Symp. Turbo Codes*, Brest, France, Sep. 2016, pp. 412–416.
- [14] S. Kudekar, T. J. Richardson, and R. L. Urbanke, "Spatially coupled ensembles universally achieve capacity under belief propagation," *IEEE Trans. Inf. Theory*, vol. 59, no. 12, pp. 7761–7813, Dec. 2013.
- [15] A. Yedla, Y. Y. Jian, P. S. Nguyen, and H. D. Pfister, "A simple proof of Maxwell saturation for coupled scalar recursions," *IEEE Trans. Inf. Theory*, vol. 60, no. 11, pp. 6943–6965, Nov. 2014.
- [16] D. G. M. Mitchell, M. Lentmaier, and D. J. Costello, "Spatially coupled LDPC codes constructed from photographs," *IEEE Trans. Inf. Theory*, vol. 61, no. 9, pp. 4866–4889, Sep. 2015.
- [17] W. Hou, S. Lu, and J. Cheng, "Spatially coupled repeater-combiner-convolutional codes," *IEEE Commun. Lett.*, vol. 20, no. 1, pp. 21–24, Jan. 2016.
- [18] K. Takeuchi, T. Tanaka, and T. Kawabata, "Improvement of BP-based CDMA multiuser detection by spatial coupling," in *Proc. IEEE Int. Symp. Inf. Theory*, St. Petersburg, Russian, Jul./Aug. 2011, pp. 1489–1493.
- [19] D. Truhachev and C. Schlegel, "Spatially coupled streaming modulation," in *Proc. IEEE Int. Conf. Commun.*, Budapest, Hungary, Jun. 2013, pp. 3418–3422.
- [20] W. K. R. Leung, G. Yue, L. Ping, and X. Wang, "Concatenated zigzag Hadamard codes," *IEEE Trans. Inf. Theory*, vol. 52, no. 4, pp. 1711–1723, Apr. 2006.
- [21] D. L. Donoho, A. Maleki, and A. Montanari, "Message-passing algorithms for compressed sensing," *Proc. Nat. Acad. Sci. USA*, vol. 106, no. 45, pp. 18914–18919, Nov. 2009.
- [22] J. Ma and L. Ping, (Feb. 2016). "Orthogonal AMP," *IEEE Access*, to be published. [Online]. Available: <https://arxiv.org/abs/1602.06509>
- [23] C.-K. Wen and K.-K. Wong, (Feb. 2014). "Analysis of compressed sensing with spatially-coupled orthogonal matrices." [Online]. Available: <https://arxiv.org/abs/1402.3215>
- [24] C. Berrou, A. Glavieux, and P. Thitimajshima, "Near Shannon limit error-correcting coding and decoding: Turbo-codes. 1," in *Proc. Conf. Rec., IEEE Int. Conf. Commun. (ICC) Geneva. Tech. Program*, Geneva, Switzerland, May 1993, pp. 1064–1070.
- [25] S. ten Brink, "Convergence behavior of iteratively decoded parallel concatenated codes," *IEEE Trans. Commun.*, vol. 49, no. 10, pp. 1727–1737, Oct. 2001.
- [26] S. Benedetto and G. Montorsi, "Unveiling turbo codes: Some results on parallel concatenated coding schemes," *IEEE Trans. Inf. Theory*, vol. 42, no. 2, pp. 409–428, Mar. 1996.